Science Advances
AAAS

advances.sciencemag.org/cgi/content/full/6/5/eaax2659/DC1

Supplementary Materials for

Single-cell analysis reveals different age-related somatic mutation profiles between stem and differentiated cells in human liver

K. Brazhnik, S. Sun, O. Alani, M. Kinkhabwala, A. W. Wolkoff, A. Y. Maslov, X. Dong, J. Vijg*

*Corresponding author. Email: jan.vijg@einsteinmed.org

Published 31 January 2020, *Sci. Adv.* **6**, eaax2659 (2020)
DOI: 10.1126/sciadv.aax2659

The PDF file includes:

Other Supplementary Material for this manuscript includes the following:

(available at advances.sciencemag.org/cgi/content/full/6/5/eaax2659/DC1)

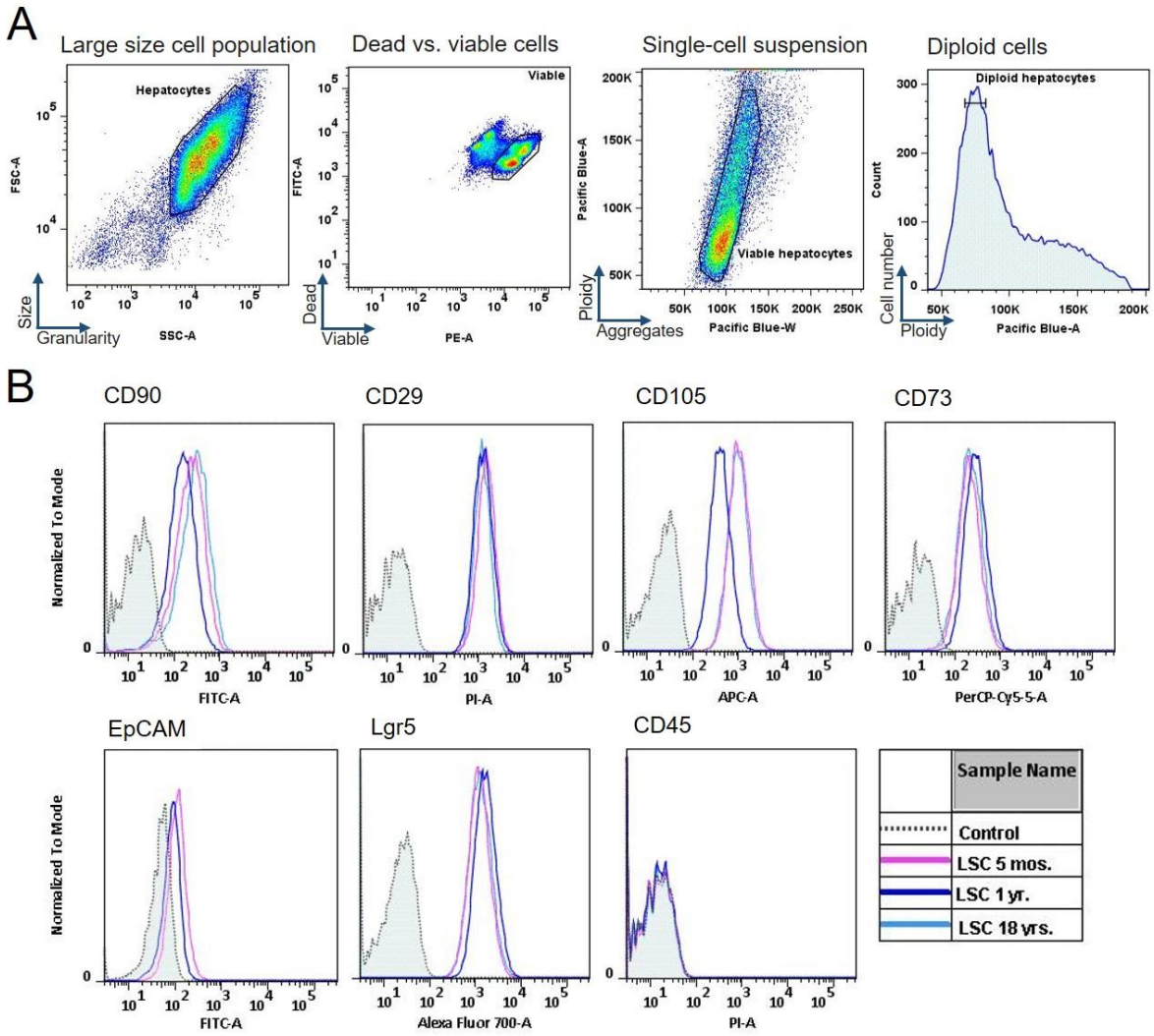

Fig. S1. Phenotypic characterization of human hepatocytes and adult LSCs by means of flow cytometry. (**A**) Typical FACS sorting layout to selectively discriminate and collect viable diploid single human hepatocytes. The example is shown for normal hepatocytes from a 77-years-old donor. Target population was selected based on large hepatocyte cell size (FSC/SSC parameters), cell viability (C_{12} Resazurin/Sytox Green) and DNA content (Hoechst 33342). (**B**) Flow cytometry analysis of control LSCs (LSC 1 yr., Kerafast, Inc.) and LSC populations (LSC 5 months, LSC 18 years) polarized and expanded from perfused hepatocyte cell fractions (Lonza Walkersville Inc.) for presence of hepatic and stem cell-specific markers (EpCAM, Lgr5, CD90, CD29, CD105, CD73) and absence of negative markers (CD45).

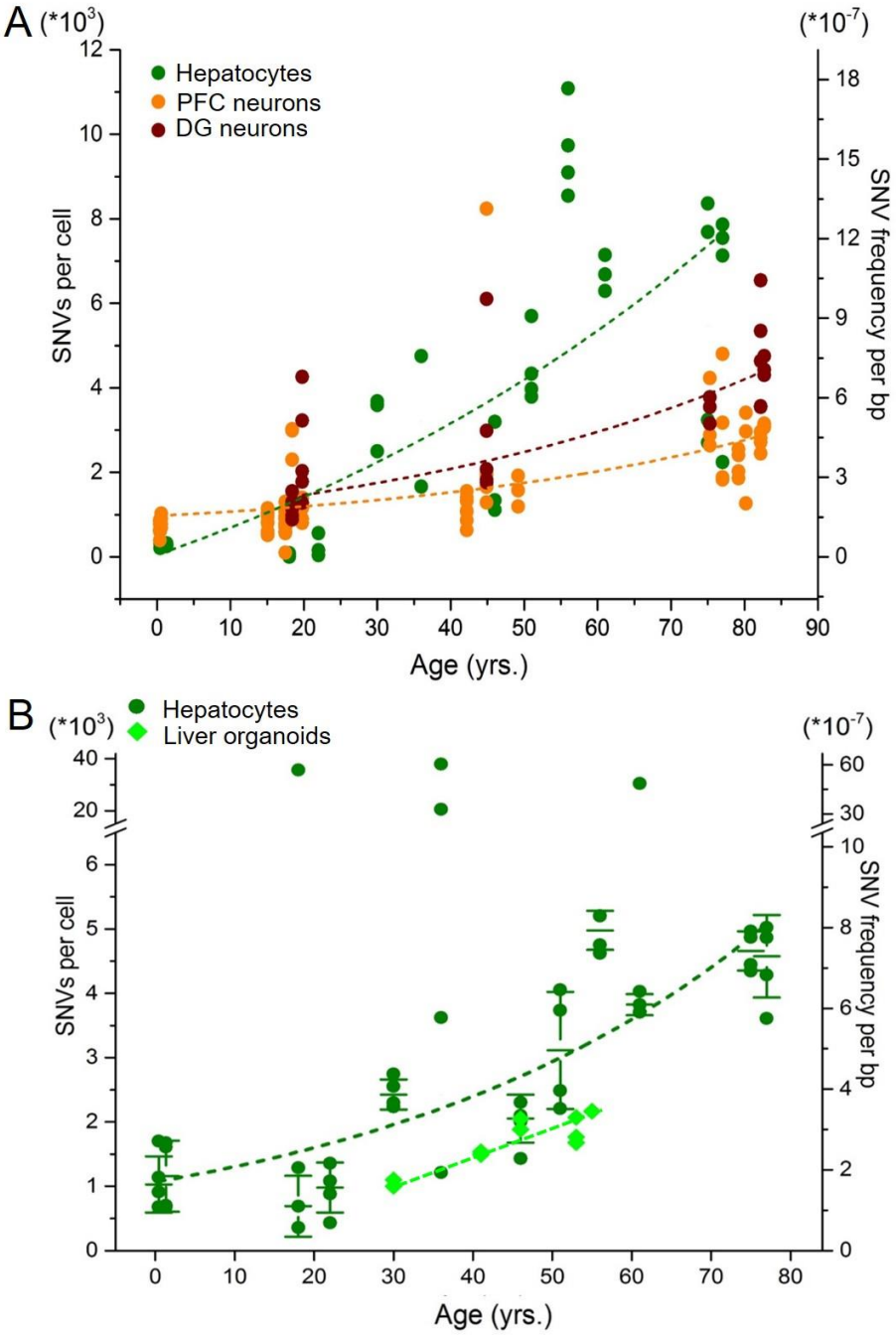

Fig. S2. Somatic mutation levels in human liver and brain. (**A**) Comparison of SNV levels in differentiated hepatocytes and neurons (prefrontal cortex (PFC) and hippocampal dentate gyrus (DG)) (*6*) identified using alternative pipeline LiRA (Linked Read Analysis). (**B**) Comparison of SNV number and frequency in human differentiated hepatocytes (dark green circles) and adult liver stem cell-derived organoids (light green diamonds) from adult/aged human donors, identified by a combination of three calling pipelines and GATK callers, respectively (*8*).

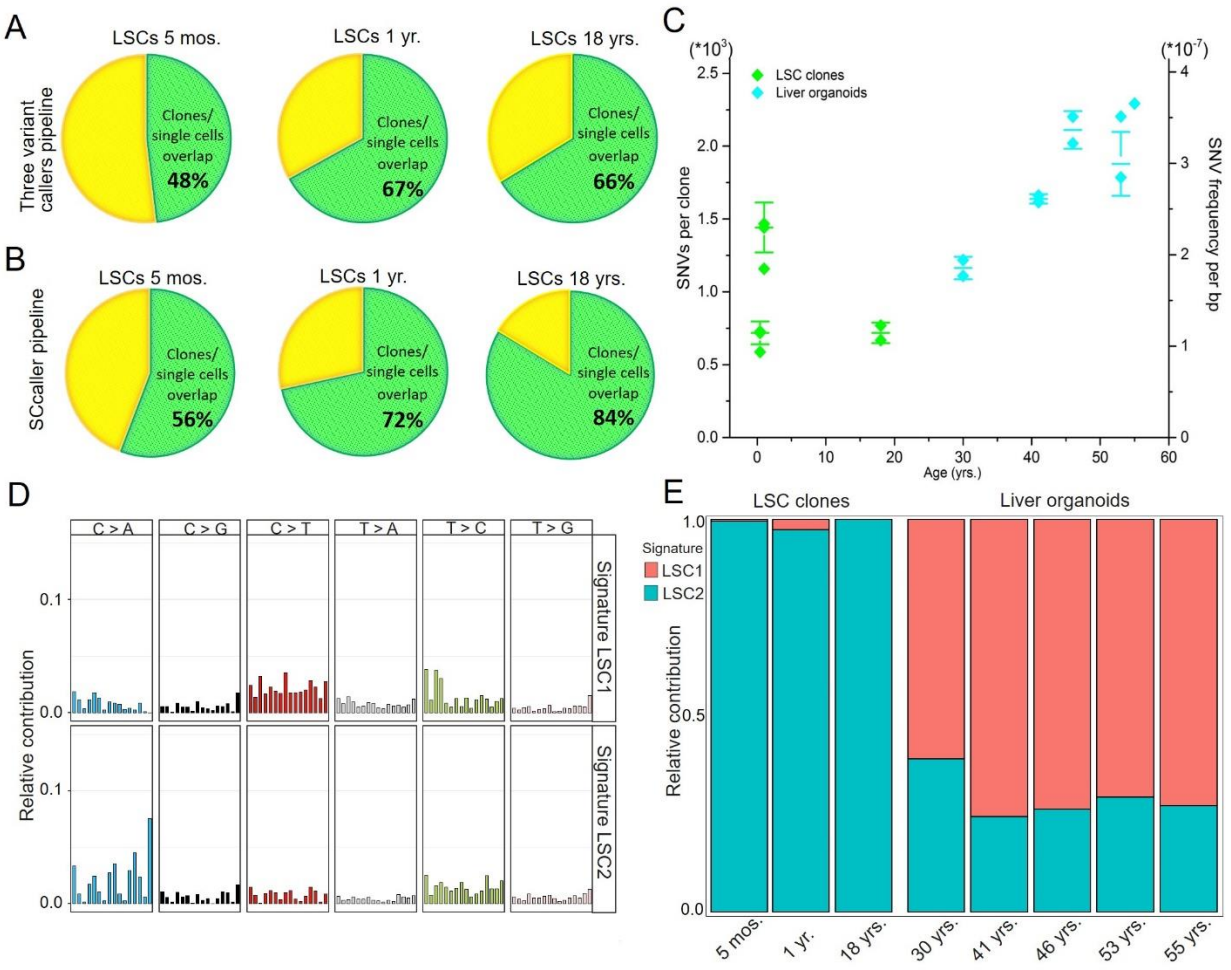

Fig. S3. Mutational landscape in LSC clones/single cells from young donors and liver organoids from adult/aged individuals (*8*). Pie charts of relative mutation fractions overlapping in LSC-derived parent clones and their kindred cells (light green) and unique for single cells only (yellow) from three young donors called by (**A**) classic combination of three pipelines and (**B**) SCcaller pipeline. (**C**) Comparison of LSC clones form three young donors (LSC 5 months, LSC 1 year, LSC 18 years; light green diamonds) with the liver-specific organoids from adult and aged donors (30-55 yrs.; light blue diamonds) (*8*). Median numbers and standard deviations among clones and organoids for each individual were calculated (light green and blue horizontal lines and vertical bars) for the statistical model. (**D**) Two mutational signatures (LSC1 and LSC2) identified by non-negative matrix factorization analysis of the somatic mutation collection observed in young adult LSC clones and adult/aged liver-specific organoids. (**E**) Contributions of liver-specific signature LSC1 and aging liver signature LSC2 to all SNVs in young adult LSC clones and adult/aged liver-specific organoids.

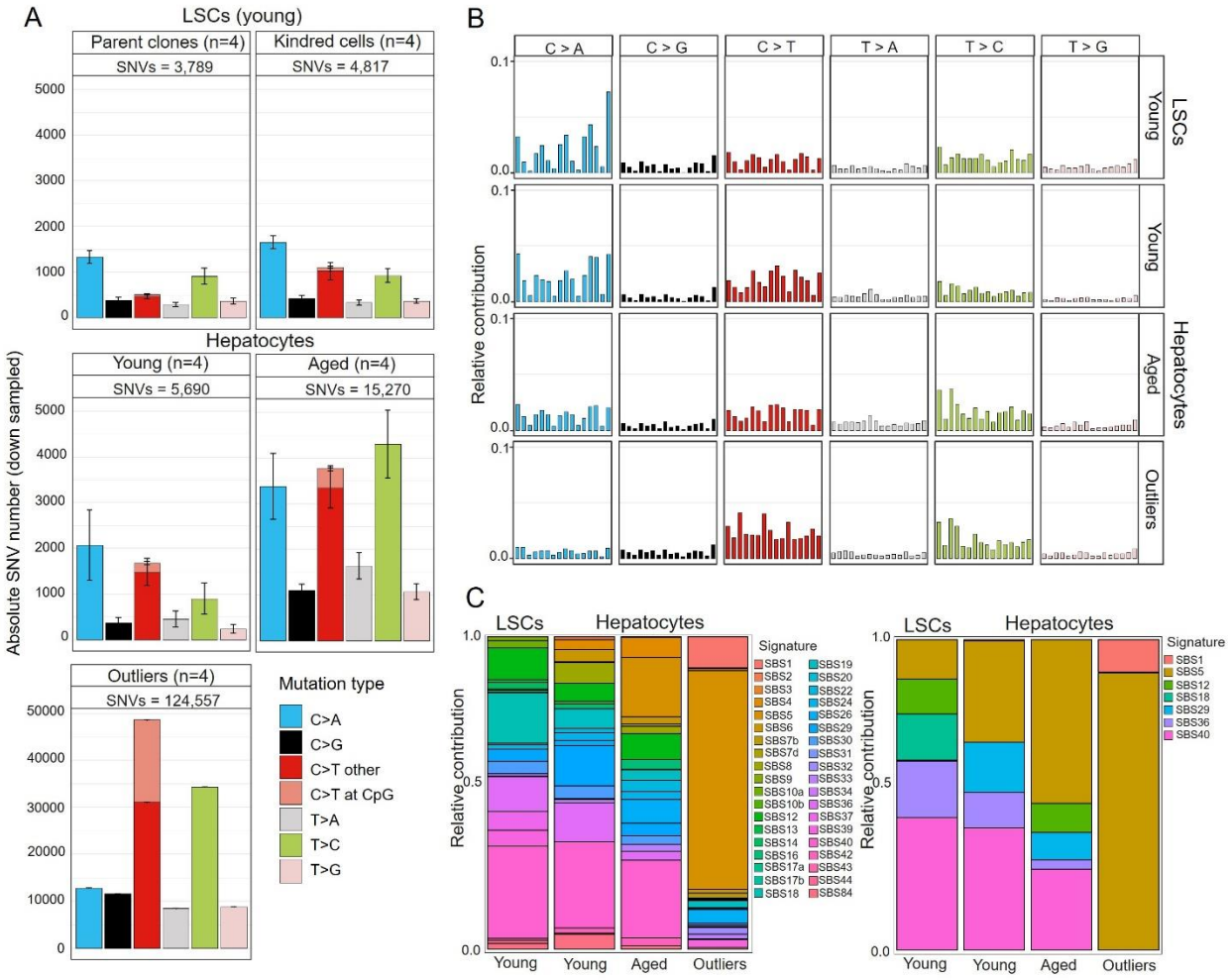

Fig. S4. Mutational spectra in human liver. (**A**) Absolute number of each of 6 indicated mutation types within 5 liver sample groups. Raw total numbers of 6 mutation types within each group were down-sampled to the same number of samples (4 cells/clones per each group extracted randomly). (**B**) The 96-mutation type profiles within different liver sample groups identified by non-negative matrix factorization analysis of the somatic mutation collection (**C**) *Left panel:* Relative contribution of the correlating COSMIC cancer signature types within different liver sample groups. *Right panel:* Relative contribution of several COSMIC signature patterns highly correlated with the mutation patterns of liver cells/groups.

Table S1. Human liver donor information list.

Table S2. Final WGS data and mutation calling results on human liver cells.

Table S3. List and description of the mutations in DNA repair–related genes identified in outlier cells with high mutation levels.

Table S4. Statistical analysis of mutation type contributions for spectra of different liver cells and groups: Pearson's χ^2 test and two-tailed Student's *t* test.

Table S5. Correlation of spectral liver group patterns and de novo signatures identified in human liver cells (L1, L2, and L3 for hepatocytes versus LSCs versus outliers and LSC1 and LSC2 for LSC cells/clones versus liver organoids) with cancer-related signatures (COSMIC) and organoid-specific signatures (*8*).

Table S6. Average number of SNVs per cell in indicated groups of pooled human liver cells distributed across total and functional liver genome within specific genome sequences.